Carbohydrate Research 345 (2010) 97–100

Contents lists available at ScienceDirect

Carbohydrate Research

journal homepage: www.elsevier.com/locate/carres

The surface structure of well-ordered native cellulose fibrils in contact with water

Erik Malm [a], Vincent Bulone [a], Kristina Wickholm [b], Per Tomas Larsson [b], Tommy Iversen [b,*]

[a] Royal Institute of Technology (KTH), School of Biotechnology, AlbaNova University Centre, SE-106 91 Stockholm, Sweden
[b] INNVENTIA AB, PO Box 5604, SE-114 86 Stockholm, Sweden

ARTICLE INFO

Article history:
Received 1 June 2009
Received in revised form 14 October 2009
Accepted 23 October 2009
Available online 30 October 2009

Keywords:
Cellulose
CP/MAS ^{13}C NMR
Spectral fitting
Halocynthia,
Gluconoacetobacter xylinus

ABSTRACT

CP/MAS ^{13}C NMR spectroscopy was used in combination with spectral fitting to examine the surface structure of hydrated cellulose I fibrils from *Halocynthia* and *Gluconoacetobacter xylinus*. To increase the spectral intensities and minimize signal overlap, *G. xylinus* celluloses site-specifically enriched in ^{13}C either on C4 or on both C1 and C6 were examined. The experimental data showed multiple C4 and C6 signals for the water accessible fibril surfaces in the highly crystalline celluloses. These signal multiplicities were attributed to structural features in the surface layers induced by the fibril interior, and could not be extracted by spectral fitting in celluloses with a lower degree of crystallinity such as cellulose from cotton.

© 2009 Elsevier Ltd. All rights reserved.

1. Introduction

The surface characteristics of cellulose fibrils have important consequences for the utilization of cellulose as a raw material for refinement to yield various polymeric and monomeric products. Fibril dimensions and the structure of cellulose chains at fibril surfaces can influence the reactivity in chemical and enzymatic hydrolysis, as well as physical phenomena such as adsorption and adhesion.

Our knowledge of the molecular arrangement at the surface of cellulose fibrils is based largely on data obtained from atomic force microscopy (AFM) applied to systems composed of highly ordered cellulose fibrils of large lateral dimensions. AFM images of the surface of cellulose fibrils from *Valonia ventricosa* immersed in water—and rich in the Iα allomorph—indicate the presence of areas with triclinic organization (Iα like), whereas areas typical of a monoclinic organization (Iβ like) have been observed for the cellulose from *Valonia macrophysa*.[1,2] The surface structure of less ordered fibrils of smaller lateral dimensions such as wood and cotton cellulose fibrils has been examined utilizing CP/MAS ^{13}C NMR spectroscopy. In the spectra obtained from these plant celluloses, two C4 signals at δ 83.3 ppm and δ 84.3 ppm have been assigned to cellulose at fibril surfaces in contact with water, one broad C4 signal at δ 83.8 ppm has been attributed to cellulose at water inaccessible surfaces formed either by interior distortions or aggregation of fibrils, and a broad cluster of C6 signals in the region of δ 62 ppm arises from the hydroxymethyl groups of the glucose residues present at the fibril surface.[3–9]

In the present study we have reinvestigated the surface structure of a set of hydrated cellulose I samples from *Halocynthia*, *Gluconoacetobacter xylinus* and cotton, using ^{13}C enrichment and CP/MAS ^{13}C NMR spectroscopy in combination with spectral fitting.

2. Experimental

2.1. Samples

Cellulose samples from cotton linters and *Halocynthia* sp. were obtained as described previously.[8]

Colonies of *G. xylinus* were cultivated on Hestrin–Schramm (HS) solid medium for 7 days at 27 °C.[10,11] Liquid cultures were obtained by inoculating 3 mL of fresh HS medium with single colonies. The liquid HS medium contained either D-glucose, D-[4-^{13}C]glucose or D-[6-^{13}C]glucose, and the cultures were grown for 14 days at 27 °C under static conditions. The cellulose film was collected and bacteria were removed by treatment with 0.1 M NaOH (aq) at 80 °C for 3 h, followed by extensive washing with de-ionized water.

* Corresponding author. Tel.: +46 8 6767210.
E-mail address: tommy.iversen@innventia.com (T. Iversen).

0008-6215/$ - see front matter © 2009 Elsevier Ltd. All rights reserved.
doi:10.1016/j.carres.2009.10.020

2.2. NMR spectroscopy

All spectra were recorded on never-dried samples (>35% water content) packed uniformly in a zirconium oxide rotor. CP/MAS ^{13}C NMR spectra were recorded at ambient temperature on a Bruker Avance AQS 300 WB instrument operating at 7.04 T. The MAS rate was in the 4–5 kHz range. A 7 mm double air-bearing probe was used. Acquisition was performed with a CP pulse sequence, using a 4.3 μs proton 90° pulse, a 800 μs ramped (100–50%) falling contact pulse and a 2.5 s delay between repetitions. A TPPM15 pulse sequence was used for ^{1}H decoupling. Glycine was used for the Hartmann–Hahn matching procedure, as well as an external standard for calibration of the chemical shift scale relative to tetramethylsilane ($(CH_3)_4Si$). The data point of maximum intensity in the glycine carbonyl line was assigned a chemical shift of 176.03 ppm.

2.3. Spectral fitting

Spectral fitting was performed as detailed elsewhere.[8,9] The software based on the Levenberg-Marquardt method[12] was developed at STFI-Packforsk.

3. Results and discussion

We previously described a procedure for analyzing molecular ordering in cellulose I fibrils, based on CP/MAS ^{13}C NMR spectra of celluloses in combination with spectral fitting of the C4 region.[5,8,9] The cross-sectional dimensions (fibril width) and bulk arrangement of the cellulose chains in fibrils from different biological sources exhibit large variations. This variability influences the features of the CP/MAS ^{13}C NMR spectra of the hydrated celluloses examined, as illustrated in Figure 1a–e. The cellulose from *G. xylinus* is composed of large well-ordered fibrils (width of about 10 nm) containing cellulose Iα and Iβ as the major and minor allomorphs, respectively. The cellulose of *Halocynthia* sp. also consists of large (width of about 11 nm), well-ordered fibrils, but cellulose Iβ is the single detectable allomorph. For the *Halocynthia* cellulose we have previously reported the presence of about 10% cellulose Iα from spectral fitting based on Lorentzian signals only.[13] However, in our refined method using both Gaussian and Lorentzian lines no cellulose Iα is detectable. In our hands it has not been possible to obtain consistent results for cellulose samples of different origins without the use of mixed line shapes for the spectral fitting procedure. Theoretical support for the need of multiple line shapes exist when spectral fitting is performed on CP/MAS spectra recorded on semi-crystalline solids such as cellulose I.[14] The cotton sample is representative for celluloses isolated from higher plants, that is, characterized by a lower allomorph content and slightly thinner fibrils (width of about 7 nm) compared to the other two celluloses examined. Table 1 compiles the lateral dimensions, fibril widths and fibril aggregate widths, as well as the proportion of cellulose allomorphs present in the different samples.

Table 1
Non-linear least-squares fittings of the C4 regions of the CP/MAS ^{13}C NMR spectra of different celluloses

Cellulose source	Iα (%)	Iβ (%)	Cr (%)	Fibril width[a] (nm)	Fibril aggregate width[a] (nm)
Gluconoacetobacter xylinus	56 (1)	22 (1)	78 (2)	10 (1)	27 (1)
Gluconoacetobacter xylinus ^{13}C enriched in C4	48 (1)	33 (1)	80 (1)	11 (0.4)	28 (2)
Gluconoacetobacter xylinus ^{13}C enriched in C6[b]	56 (3)	22 (2)	78 (4)	10 (0.4)	28 (2)
Halocynthia sp.	nd	69 (1.2)	69 (1.2)	11 (0.7)	38 (5.5)
Cotton linters	32 (0.6)	6 (0.3)	38 (0.8)	7 (0.1)	40 (1.3)

Cr = total allomorph content; nd = not detectable. Values given in parentheses are standard errors.
[a] Fibril and fibril aggregate widths were calculated assuming square cross-sections.
[b] The fitting was from the C6 region.

3.1. Spectral fitting of the C4 region

The spectral C4 region representing the cellulose chains located in the fibril interior (δ 86–92 ppm) typically yields signals of high signal-to-noise ratios (Fig. 1). However, the large cross-sectional dimensions of the *Gluconoacetobacter* and *Halocynthia* celluloses

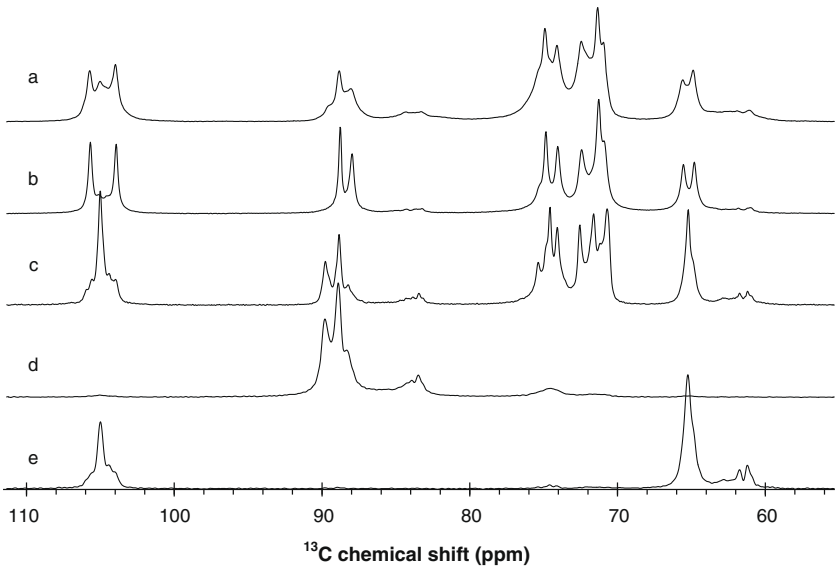

Figure 1. CP/MAS ^{13}C NMR spectra of cellulose samples from (a) cotton, (b) *Halocynthia*, (c) *Gluconoacetobacter xylinus*, (d) *Gluconoacetobacter xylinus* enriched in ^{13}C at the C4 position, and (e) *Gluconoacetobacter xylinus* enriched in ^{13}C at the C1 and C6 positions.

result in very low intensities for the signals in the C4 region originating from the cellulose chains located at fibril surfaces (δ 80–86 ppm). A further complication is the presence of fibril aggregates. The fibril aggregates contain fibril-to-fibril contact surfaces which, together with internal fibril distortions, give surfaces that are inaccessible to water and appear as a broad Gaussian signal at or close to δ 84 ppm upon spectral fitting. Spectral fitting of the C4 surface region of the well-ordered cellulose from *Halocynthia*, which contains only the Iβ allomorph, demonstrates a pattern of four signals (δ 83.3, δ 83.7, δ 84.3 and δ 84.9 ppm) of nearly equal intensity from water accessible surfaces, using Gaussian line shapes (Fig. 2). This multiplicity may be related to the monoclinic organization (Iβ like) of surface cellulose, as observed in AFM images of *V. macrophysa* fibrils.[1] The surface chains in the *Halocynthia* cellulose are in contact with the crystalline interior and could be arranged in a manner resembling a two-chain monoclinic crystalline phase with cellobiose repeating units.

The well-ordered cellulose from *G. xylinus* enriched in ^{13}C on the C4 position, and containing both cellulose Iα and Iβ, exhibits five ^{13}C NMR signals originating from the accessible surfaces (Fig. 2). Most of the signals reproduce, within experimental error, the signal position and relative intensities found for the C4 surface signals in the *Halocynthia* cellulose. The main difference is an additional signal of relatively high intensity at δ 83.5 ppm for the *G. xylinus* cellulose. We have previously observed such a high intensity signal in spectra of cellulose samples rich in the Iα allomorph from the algal species *V. ventricosa* and *Cladophora* sp.[5,15] An explanation of the relatively broad (FWHH 1.5 ppm) signal at δ 83.5 ppm could be related to a triclinic organization (one chain) of surface cellulose, as observed earlier in AFM images of *V. ventricosa* fibrils rich in the Iα allomorph.[2] A combination of monoclinic and triclinic organization of the surface cellulose is further substantiated by comparison of the Iα/Iβ ratios which are 1.5 and 2.6, respectively, in the fibril interior and surface cellulose of ^{13}C4-enriched cellulose from *G. xylinus*. Even if this does not give an exact agreement in the ratios, the trend is the same, that is, a dominance of the Iα allomorph.

In the less ordered cotton cellulose the C4 accessible surface signals coalesce into two signals or signal clusters at δ 83.3 and δ 84.3 ppm.[5] In the cotton cellulose, the content of the Iα (6%) and Iβ (32%) allomorphs in the fibril is too low to give a completely crystalline interior which theoretically would require a Iα and Iβ content near 70%, based on an average fibril width of 7 nm.[5] Instead we observe a substantial amount of *para*-crystalline cellulose (30%) probably also in contact with the surface chains, resulting in a loss of the fine structure in the C4 surface signals.[5,8] This behavior is expected if the C4 signals of water accessible surfaces in hydrated cellulose fibrils reflect in part the underlying structure in the fibril interior. However, in a highly ordered system lacking any detectable presence of *para*-crystalline cellulose surface chains reside directly on top of a crystalline lattice resulting in a more resolved signal pattern. This is the case observed for surface signals from well-ordered cellulose fibrils such as those from *G. xylinus*, which contain substantial quantities of both the Iα and Iβ allomorphs (Table 1). Hence the different spectral features of the surface signals detected in cotton cellulose and in cellulose from *G. xylinus* can be explained in terms of different system properties mediated by the same mechanism. Although inhomogeneous line broadening is the most probable cause for the structural effects on spectra, similar influences have recently been observed for the dynamic properties of fibril surface chains by analyzing experimental ^{13}C T_1 relaxation times using molecular dynamics (MD) simulations.[16] The MD simulations could explain the different relaxation times observed for the two surface signals in cotton linters (δ 83.2 and δ 84.3 ppm) in terms of the different underlying crystallographic planes.

3.2. Spectral fitting of the C6 region

To investigate the C6 surface signals in more detail, *G. xylinus* was cultivated in the presence of D-[6-^{13}C]glucose. Transfer of ^{13}C labeling from C6 to C1 during biosynthesis of cellulose in *G. xylinus* grown in the presence of D-[6-^{13}C]glucose has been reported earlier.[11] In our case, nearly half of the original ^{13}C-6 labeling was found on the C1 position after culture (Fig. 1). However, the spectrum gave a low noise signal cluster of C6 signals from interior and surface chains. It should be noted that spectral fitting of the C-6 signals resulted in the same average lateral fibril and fibril aggregate dimensions and allomorph compositions as spectral fitting of the C4 signals in the unlabeled *G. xylinus* cellulose (Table 1). In Figure 3, the C-6 signals corresponding to water accessible surfaces as obtained by spectral fitting are shown. For the rest of the celluloses investigated, the C-6 signals could not be separated by spectral fitting but it is apparent from the spectral features that there exist signal intensities at positions similar to those observed in the *G. xylinus* cellulose (Fig. 4). Analysis of the spectrum corresponding to the ^{13}C6-enriched *G. xylinus* cellulose reveals three signals of nearly identical intensities at δ 61.0, δ 61.2, and δ 61.7 ppm. The positions of these signals are all within the range 60–62 ppm proposed for the gauche–gauche conformation of the hydroxy-

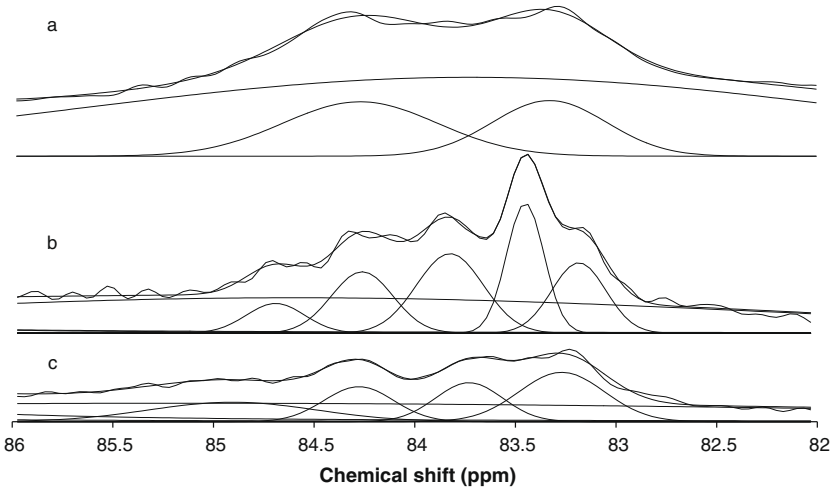

Figure 2. Spectral fitting of the C4 surface region from (a) cotton, (b) *Gluconoacetobacter xylinus* enriched in ^{13}C at the C4 position, and (c) *Halocynthia*.

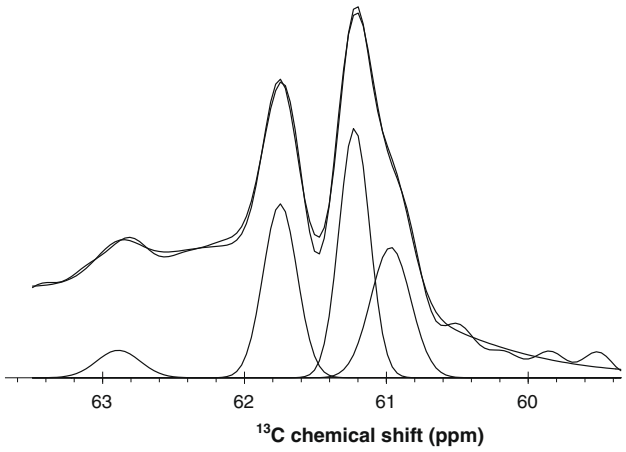

Figure 3. Spectral fitting of the C6 surface region from *Gluconoacetobacter xylinus* cellulose enriched in ^{13}C at the C6 position. Only the fitted functions corresponding to water accessible surfaces are shown, the function corresponding to inaccessible fibril surfaces is omitted for clarity.

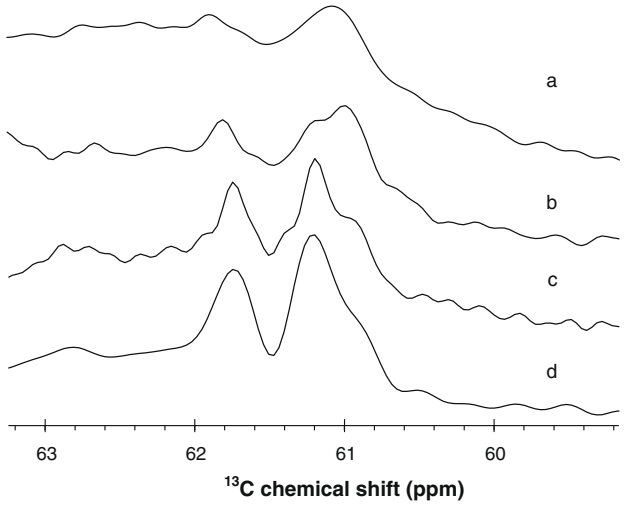

Figure 4. Enlargements of the C6 surface region of cellulose samples from (a) cotton, (b) *Halocynthia*, (c) *Gluconoacetobacter xylinus*, and (d) *Gluconoacetobacter xylinus* enriched in ^{13}C at the C6 position.

methyl group.[7,17,18] The reason for three different gauche–gauche signals is not obvious from the spectrum, but could be related to the hydroxymethyl group pointing either toward the water phase or the fibril interior and to differences in the hydrogen bonding pattern as shown in recent computer simulations of cellulose Iβ.[19] In addition, the small signal observed at δ 62.9 ppm could be attributed to the gauche–trans conformer of the hydroxymethyl group. In the cotton cellulose that contains substantial amounts of *para*-crystalline cellulose (30%) a major part of the fine structure of both the C4 and C6 signal clusters is missing.

4. Conclusions

The structure of the surface of well-ordered hydrated cellulose fibrils such as those from *Halocynthia* and *G. xylinus* can be described by a model involving both water accessible surface signals, which partially reflect the underlying interior allomorph structure (Iα and Iβ), and a distorted water inaccessible C4 signal, which arises as a consequence of fibril aggregation and/or defects in the fibril interior when such are present. For the C6 signal cluster, water accessible and inaccessible surface signals are observed, but the fine structure is given by the conformation of the hydroxymethyl group and dominated by three signals in the range 61–62 ppm recently attributed to gauche–gauche conformers. In the less ordered cotton cellulose containing a substantial amount of *para*-crystalline cellulose, a major part of the fine structure of both the C4 and C6 signal clusters is lost.

Acknowledgment

This work was supported by the Swedish Centre for Biomimetic Fibre Engineering (www.biomime.org).

References

1. Kutti, L.; Peltonen, J.; Pere, J.; Teleman, O. *J. Microsc.* **1995**, *178*, 1–6.
2. Baker, A. A.; Helbert, W.; Sugiyama, J.; Miles, M. J. *Biophys. J.* **2000**, *79*, 1139–1145.
3. Newman, R. H.; Hemmingson, J. A. *Cellulose* **1994**, *2*, 95–110.
4. Wormald, P.; Wickholm, K.; Larsson, P. T.; Iversen, T. *Cellulose* **1996**, *3*, 141–152.
5. Wickholm, K.; Larsson, P. T.; Iversen, T. *Carbohydr. Res.* **1998**, *312*, 123–129.
6. Newman, R. H. *Holzforschung* **1998**, *52*, 157–159.
7. Horii, F.; Hirai, A.; Kitamaru, R. *Polym. Bull.* **1983**, *10*, 357–361.
8. Larsson, P. T.; Wickholm, K.; Iversen, T. *Carbohydr. Res.* **1997**, *302*, 19–25.
9. Larsson, P. T.; Hult, E.-L.; Wickholm, K.; Pettersson, E.; Iversen, T. *Solid-State NMR* **1999**, *15*, 31–40.
10. Hestrin, S.; Schramm, M. *Biochem. J.* **1954**, *58*, 345–352.
11. Arashida, T.; Ishino, T.; Kai, A.; Hatanaka, K.; Akaike, T.; Matsuzaki, K.; Kaneko, Y.; Mimura, T. *J. Carbohydr. Chem.* **1993**, *12*, 641–649.
12. Press, W. H.; Flannery, B. P.; Teukolsky, S. A.; Vetterling, W. T.. *Numerical Recipes, The Art of Scientific Computing*; Cambridge University Press: Cambridge, 1988.
13. Larsson, P. T.; Westermark, U.; Iversen, T. *Carbohydr. Res.* **1995**, *278*, 339–343.
14. Larsson, P. T.; Westlund, P.-O. *Spectrochem. Acta, Part A* **2005**, *62*, 539–546.
15. Wickholm, K. Structural Elements in Native Celluloses, Doctoral Thesis, Royal Institute of Technology, Stockholm, Sweden, 2001.
16. Bergenstråhle, M.; Wohlert, J.; Larsson, P. T.; Mazeau, M.; Berglund, L. A. *J. Phys. Chem. B* **2008**, *112*, 2590–2595.
17. Viëtor, R. J.; Newman, R. H.; Ha, M.-A.; Apperley, D. C.; Jarvis, M. C. *Plant J.* **2002**, *30*, 721–731.
18. Newman, R. H.; Davidson, T. C. *Cellulose* **2004**, *11*, 23–32.
19. Matthews, J. F.; Skopec, C. E.; Mason, P. E.; Zuccato, P.; Torget, R. W.; Sugiyama, J.; Himmel, M. E.; Brady, J. W. *Carbohydr. Res.* **2006**, *341*, 138–152.